COBEM 2023 27TH INTERNATIONAL CONGRESS OF MECHANICAL ENGINEERING

ABCM Brazilian Society of Mechanical Sciences and Engineering
27th ABCM International Congress of Mechanical Engineering
December 04-08, 2023, Florianópolis-SC, Brazil

COB-2023-2302
Flight Campaign Analysis of a Flexible Wing UAV for Studying Flexible Aircraft Dynamics

Vítor Paixão Fernandes
Thiago Rosado de Paula
Rodrigo Costa do Nascimento
Luiz Carlos Sandoval Góes
Roberto Gil Annes da Silva
ITA - Instituto Tecnológico de Aeronáutica, 12228-900, São José dos Campos, Brasil
vitor.paixao@ga.ita.br, thiagorp@ita.br, rodrigo.nascimento@ga.ita.br, goes@ita.br, gil@ita.br

Alain Gomes de Souza
IDMEC, Instituto Superior Técnico, Universidade de Lisboa, 1049-001, Lisboa, Portugal
alain.souza@tecnico.ulisboa.pt

Abstract. *This article presents an analysis of a flight campaign using a small flexible wing UAV. The aircraft has a 4m wingspan, an aspect ratio of 18.9, electric propulsion, and an acquisition system that permits studying the effects of flexibility. Flights were performed to evaluate the behavior of the system concerning the data acquisition system, and excitations were conducted to obtain responses for specific modes. To ensure precise time and amplitude control of the inputs and to remove problems associated with manual execution, programmed maneuvers were used. Data compatibility was verified using the flight path reconstruction (FPR) technique. The paper also discusses the effects of wing flexibility on sensor measurements that do not aim to be related to flexible modes and operational aspects of the test flights. The results of the FPR analysis showed that the recorded data is consistent and the evaluated biases, scale factors and time delays obtained with the FRP were able to correlate the recorded data with the model, except for airspeed and angle of attack, which were not well fitted with the classic rigid body kinematics. The system proved to be an effective platform for studying flexible aircraft flight dynamics, and the established procedure to execute inputs and their respective recorded response provided a solid foundation for further research using this platform, improving past campaigns that relied on manual inputs.*

Keywords: *Flexible Aircraft, UAV, Flight Dynamics, FPR, Identification.*

1. INTRODUCTION

Obtaining an accurate model for an aircraft is an essential step in the development of flight dynamics simulations, control systems, failure analysis, and associated constraints, among other applications. The demand for precise modeling of flexible aircraft dynamics has increased with the advent of large and energy-efficient aircraft (Deiler *et al.*, 2023). In recent decades, various mathematical formulations have emerged to represent aircraft's flight dynamics. These methodologies differ in their fidelity to capturing the intricacies of flight physics, structural dynamics, aerodynamics, or their interplay (Zuñiga *et al.*, 2020).

In this context, enhancing the model's fidelity with aircraft physics can be achieved through the identification of dynamic systems. This process involves retrieving information about the aircraft using operational data, which is obtained during its flights. Research has already been conducted to estimate key parameters for both rigid and flexible aircraft models through identification. These investigations have been carried out in both the time and frequency domains, with the primary goal of estimating stability derivatives (de Paula *et al.*, 2023), (Grauer and Boucher, 2020),(Deiler *et al.*, 2023). The utilization of these parameter estimation approaches consistently yields favorable outcomes in constructing mathematical models.

The latest generation of aircraft often exhibits lower natural frequencies in their initial structural modes, which leads to interactions with rigid-body responses, challenging the conventional separation between independent rigid-body flight mechanics and structural motion (Deiler *et al.*, 2023). Therefore, the identification of parameters for flexible aircraft models increases in interest, and it has been accomplished through a combination of rigid-body and structural dynamics, a concept proposed by Waszak and Schmidt (1988) and shown to be feasible using the output error model in the time domain by Silva and Monnich (2012).

To advance with the system parameter identification of an aircraft, it is imperative to conduct experimental tests. This article primarily focuses on the operational aspects of a flight campaign involving a small flexible-wing UAV while pre-

senting results pertaining to the initial steps of parameter identification. As mentioned earlier, there are various compelling reasons to explore flexible aircraft flight dynamics. The development of methodologies for analyzing flexible unmanned small aircraft is particularly attractive due to their cost-effectiveness, versatility, and potential for specific applications.

2. FLIGHT TEST PLATFORM

The plane used in the study was a 4m wingspan UAV named EOLO, built to be used as a test platform regarding flexible aircraft studies for the Laboratory of Aeronautical Systems (LSA) of the Aeronautics Institute of Technology (ITA). The aircraft is shown in Fig. 1 and is based on the FT-100 Horus, a UAV developed and built by the FT Sistemas company, designed to operate surveillance missions and military purposes. The main difference from the military commercial model is a custom-made flexible composite wing. Table 1 summarizes the main parameters of EOLO.

Figure 1. Aircraft in the takeoff configuration.

Table 1. EOLO UAV main characteristics.

Parameter	Value
Wing Area	0.85 m²
Wing Chord	0.23 m²
Wingspan	4.00 m
Wing Aspect Ratio	18.9
Total Length	1.89 m
Total Mass	9.4 kg

2.1 Data acquisition system

The aircraft control and data acquisition system is based on a flight computer developed by the aircraft manufacturing company. The computer receives the radio control inputs via a radio receiver, sends signals to actuate the servo motors of the flight controls and has a telemetry link to a ground station. This system can be used in a closed loop, which was not the case in this work. The computer relies on data acquired from an inertial measuring system (INS), which provides accelerations and angular velocities, Euler angles, airspeed, anemometric altitude and GNSS data, among other information. The military aircraft has other systems, that are not present in the flexible EOLO, but the flexible aircraft also incorporates a secondary system to further obtain other important variables to the flexibility analysis.

This secondary system communicates and receives data from the primary system while also obtaining data from a data boom, used to measure the angle of attack (α) and angle of sideslip (β). In addition to those sensors, the aeroelastic acquisition system also has accelerometers and strain gauges, whose data can be used to identify the model including the effects of the structure dynamics response during flight, as the sensor's outputs are composed by the dynamics of the rigid-body and the motion of the structure (Silva, 2018). Figure 2 presents the accelerometer and extensometer sensor distribution in the aircraft body.

2.2 Radio control system and operation

The aircraft is always flown in line of sight and does not have a video transmission system. It has a radio transmitter that the pilot uses to control the aircraft in pilot in control (PIC), also referred to as manual mode, and to switch between PIC and computer in control (CIC), also named closed loop. This radio transmitter does not provide resources to program inputs, so in PIC the pilot must manually generate all the controls using the sticks or a switch to change between predetermined values, whose timed change is made by the pilot. However, like most commercial radio transmitters, it has a PPM signal connector used to allow for trainer mode, which permits transmitting the inputs from another radio. So, to surpass

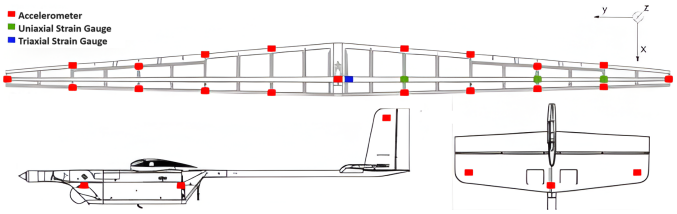

Figure 2. Accelerometers and strain gauges position (Souza *et al.*, 2023).

the limitation of manually executed inputs, aiming to give the system precisely timed inputs, an additional radio control was used, this one allowing its output signal to be programmed via scripts. Those scripts are executed while a momentary switch is held by the pilot allowing the radio control to perform the maneuver and send the signal to the first transmitter (master).

All the maneuvers contain three steps, which are:

1. Maintain the inputs that trimmed the aircraft in the desired condition for a determined time.
2. Execute the predetermined maneuver.
3. Return the inputs that trimmed the aircraft before the maneuver begins for a determined time.

The sequence maneuver is coordinated between both pilots in the following manner:

1. First pilot flies the aircraft and trims it to the desired velocity and altitude to perform the maneuver using the master radio. The ground personnel checks the desired values via the telemetry data.
2. When the aircraft is trimmed in the desired condition, the first pilot holds a momentary switch which allows the second radio inputs to be sent to the aircraft.
3. While the first pilot holds the switch, the second pilot also activates and holds a momentary switch that executes the maneuver sequence, as described before.
4. When the sequence ends, the first pilot releases the transfer switch and retrieves control of the aircraft. If the switch of the master radio continues to be pressed, the second pilot can control the aircraft using his radio control sticks.

At any given moment the second pilot can act on the sticks of the slave radio to override the preconfigured inputs and if the switch is released the commands return to the trimmed ones in the beginning. Furthermore, if the first pilot releases the switch, the inputs are given to him independent of the ones on the second radio. Figure 3 summarizes the radios setup.

The main advantage to this approach is the fact that the operation can be done using two pilots, one focused on piloting the aircraft during the flight and the other monitoring the instrument status and executing the programmed maneuvers, which makes it easier to have better results regarding the execution and achieving trimmed conditions for different altitude and speed. Besides that, the radio controllers used are the same type that the pilots are used to in general radio-controlled aircraft operations. Furthermore, the proven and reliable radio control system of the full carbon fuselage aircraft does not need to be changed. At the same time, new resources can be added using more modern flexible solutions.

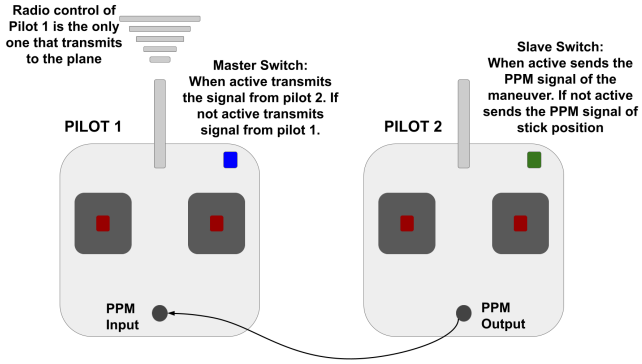

Figure 3. Radio control diagram.

3. SYSTEM IDENTIFICATION

The Quad-M methodology was the foundation for constructing the flight test campaigns, deriving its name from four key elements: maneuver, measurements, method, and model. Carefully planned maneuvers are needed to excite different system modes, requiring sufficient energy in each of the frequencies of the desired modes. To record the system dynamics, the measurements must provide highly accurate data for the selected variables. Finally, a suitable method must be chosen to yield high-quality results, considering all the major aspects of the model and its dynamics (Jategaonkar, 2015). Zúñiga (2019) developed the optimized inputs to study the EOLO dynamics, for the flexible and rigid body modes, which were the maneuvers performed during the flight campaign.

The model employed in the identification procedure represents the flight dynamics of the aircraft and it must encompass the effects of flexibility. Therefore, besides the typically executed rigid body vehicle identification, where stability and control derivatives are the primary identification parameters, there are other parameters to account for regarding flexibility and its effects (Silva, 2018).

In order to develop the identification in the time domain, the commonly used methods are the output error (OEM), filter error (FEM) and equation error (Jategaonkar, 2015). A comparison was done by Silva (2018) about the application of the FEM and the OEM to the identification of a flexible aircraft in the time domain, and the chosen method was the OEM, as in relation to the FEM it can be used in data provided with different process noise characteristics, which might occur as the campaigns can consist of many flights during the time span of various days. Furthermore, Silva (2018) stated that the filter error using the Kalman filter or extended Kalman filter could have a good match even with critical modeling errors, which will be evaluated by the method as process noise. This characteristic can bring difficulties in concluding about a valid procedure of identification or the validation of the adopted model.

The method adopted in this work is the output error, a procedure applied to parameter identification systems that permit the estimation of parameters by iteratively adjusting them in order to minimize a computed error between the computed model responses using those parameters and the measured variables. This method can only deal with measurement noises, not process noise (Jategaonkar, 2015).

Figure 4 and 5 show the diagram for both the 4-M method and the OEM.

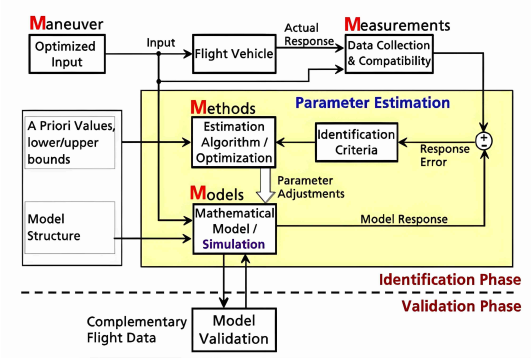

Figure 4. Quad-M methodology diagram (Jategaonkar, 2015).

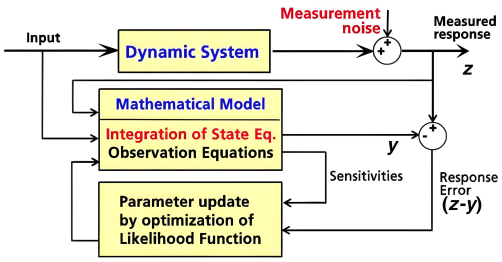

Figure 5. Output error method diagram (Jategaonkar, 2015).

3.1 Flight Path Reconstruction (FPR)

Accomplishing a confirmation of the agreement between the physical model and the data collected by the sensor can be done with the flight path reconstruction (FPR). FPR is a data compatibility check used to validate the gathered sensor data according to the system model and kinematics and can be used to obtain the systematic errors present in the instrumentation (Jategaonkar, 2015).

The Eq. 1 presents a generic model described by Jategaonkar (2015) for modeling a sensor accounting for the bias (Δy), scale factor (K_y) and time delay (τ) and was used in this work. The subscript c refers to the corrected value, while m refers to the recorded sensor data. The FRP permits obtaining those corrections for a given sensor. The time delay might relate to the acquisition system and can originate from a timing mismatch between computed variables calculated and communicated by different sensors or subsystems, as is the case of the EOLO that has more than one acquisition system, but also to unsteady aerodynamics effects, for example.

$$y_c(t) = K_y y_m(t - \tau) + \Delta y, \tag{1}$$

The physical model applied through this step was the rigid-body classical kinematics, using the assumption that the inertial measurement unit (IMU), which is mounted in the fuselage central section, with increased rigidity when compared with the other parts of the aircraft structure, while being placed close to the CG, will not be further influenced by the flexible structural dynamics (Silva, 2018). The kinematics equations described by Jategaonkar (2015) are present in Eq. 2. Those expressions permit the determination of the state variables with the IMU data of the aircraft, and do not have any direct dependence on the aerodynamics variables measurements, as their contribution is related to the forces in x, y and z axis that induce the accelerations, being those used to the FPR (Jategaonkar, 2015).

$$\begin{aligned}
\dot{u} &= -qw + rv - g\sin(\theta) + a_x^{CG}, \\
\dot{v} &= -ru + pw - g\cos(\theta)\sin(\phi) + a_y^{CG}, \\
\dot{w} &= -pv + qu - g\cos(\theta)\cos(\phi) + a_z^{CG}, \\
\dot{\phi} &= p + q\sin(\phi)\tan(\theta) + r\cos(\phi)\tan(\theta), \\
\dot{\theta} &= q\cos(\theta) - r\sin(\phi), \\
\dot{\psi} &= (q\sin(\phi) + r\cos(\phi))\sec(\theta), \\
\dot{h} &= u\sin(\theta) - v\sin(\phi)\cos(\theta) - w\cos(\theta)\cos(\phi),
\end{aligned} \tag{2}$$

In Eq. 2, u, v and w are the velocities in the aircraft body axes, the Euler angles ϕ and θ are the roll and pitch angles in the aircraft body axes, and h is the height. The yaw angle (ψ), not present in the kinematics, as the x and y positions are not being used, is described together with ϕ and θ in Eq. 3. The a_x^{CG}, a_y^{CG} and a_z^{CG} are the linear accelerations in the center of gravity. The p, q and r are the rotational velocities around the body axis and can be computed as described in Eq. 4.

$$\begin{aligned}
\phi &= k_\phi \phi_m - \Delta\phi, \\
\theta &= k_\theta \theta_m - \Delta\theta, \\
\psi &= k_\psi \psi_m - \Delta\psi,
\end{aligned} \tag{3}$$

$$\begin{aligned}
p &= k_p p_{IMU} - \Delta p, \\
q &= k_q q_{IMU} - \Delta q, \\
r &= k_r r_{IMU} - \Delta r,
\end{aligned} \tag{4}$$

As there are position offsets on the instrumentation system in relation to the center of gravity (CG), relative to the body axis, they must be used in the FPR computations and are present in Tab. 2 for the EOLO UAV.

Table 2. Flight Instrumentation Offsets.

Instrument	**x (m)**	**y (m)**	**z (m)**
IMU	0.010	0.000	0.012
α Vane	0.120	0.400	-0.110
β Vane	0.059	0.400	-0.110
Pitot tube	0.059	-0.400	-0.090

The calculation of the linear accelerations in the CG, accounting for the position offset of the IMU, the bias and scale factors can be done using Eq. 5. If misalignment on an accelerometer system is present and not taken into account previously in a laboratory calibration, the measurements in one axis would be influenced by values of the other axis

and extended corrections must be made (Jategaonkar, 2015). The missing time derivatives $\dot{p}$,$\dot{q}$ and $\dot{r}$ are obtained from numerical differentiation from the angular rates p,q and r.

$$\begin{aligned} a_x^{CG} &= k_{ax}a_x^{IMU} + (q^2+r^2)x_{IMU} - (pq-\dot{r})y_{IMU} - (pr+\dot{q})z_{IMU} - \Delta a_x, \\ a_y^{CG} &= k_{ay}a_y^{IMU} - (pq+\dot{r})x_{IMU} - (p^2+r^2)y_{IMU} - (qr-\dot{p})z_{IMU} - \Delta a_y, \\ a_z^{CG} &= k_{az}a_z^{IMU} - (pr+\dot{q})x_{IMU} - (qr+\dot{p})y_{IMU} + (p^2+q^2)z_{IMU} - \Delta a_z, \end{aligned} \tag{5}$$

The computation of the local velocities in the pitot tube position can be done using Eq. 6. It is analogous for the u_α, v_α, w_α and u_β, v_β, w_β local velocities in α and β vanes positions, considering their respective offsets.

$$\begin{aligned} u_{pt} &= u - ry_{pt} + qz_{pt}, \\ v_{pt} &= v - pz_{pt} + rx_{pt}, \\ w_{pt} &= w - qx_{pt} + py_{pt}, \end{aligned} \tag{6}$$

The measurement values can be calculated as shown in Eq. 7. The subscript indicates a time shift in the variable, as stated in Eq. 1.

$$\begin{aligned} V_m &= \sqrt{u^2+v^2+w^2}, \\ \alpha_m &= k_\alpha \arctan(w_\alpha/u_\alpha)_{\tau_\alpha} + \Delta\alpha, \\ \beta_m &= k_\beta \arcsin(v_\beta/\sqrt{u_\beta^2+v_\beta^2+w_\beta^2})_{\tau_\beta} + \Delta\beta, \\ \phi_m &= k_\phi\phi_{\tau_\phi} - \Delta\phi, \\ \theta_m &= k_\theta\theta_{\tau_\theta} - \Delta\theta, \\ \psi_m &= k_\psi\psi_{\tau_\psi} - \Delta\psi, \\ h_m &= h, \end{aligned} \tag{7}$$

All the information about the FPR, states, observations and parameters are present in Tab. 3 and Tab. 4.

Table 3. Flight path reconstruction information.

Category	**Variables**
States	$u, v, w, \phi, \theta, \psi, h$
Inputs	$p_{\text{IMU}}, q_{\text{IMU}}, r_{\text{IMU}}, a_x^{\text{IMU}}, a_y^{\text{IMU}}, a_z^{\text{IMU}}$
Measurements	$V, \alpha, \beta, \phi, \theta, \psi, h$

Table 4. Flight Path Reconstruction Correction Parameters.

Category	**Parameters**
Biases	$\Delta a_x, \Delta a_y, \Delta a_z, \Delta p, \Delta q, \Delta r, \Delta\alpha, \Delta\beta, \Delta\phi, \Delta\theta, \Delta\psi$
Scale Factors	$k_{ax}, k_{ay}, k_{az}, k_p, k_q, k_r, k_\alpha, k_\beta, k_\phi, k_\theta, k_\psi$
Time Delays	$\tau_\alpha, \tau_\beta, \tau_\phi, \tau_\theta, \tau_\psi$

It was also assumed that the α and β vanes were fixed in a section of the aircraft that does not have deflections that could lead to a big influence of the flexible dynamics in the measurements, so those variables would be only related to the rigid body dynamics.

All the data analysis was developed in Matlab, and the FPR was executed based on software formulation provided by Jategaonkar (2015).

4. FLIGHT DATA, FPR AND IDENTIFICATION RESULTS

EOLO has been flown through flight campaigns that involve the necessary steps for flight identification, following maneuvers and ensuring that the data acquisition could measure all the required variables. The first campaign was executed when the plane did not have aerodynamic vanes installed, then the vanes were installed and the aircraft flew for a second campaign. The results from the data analysis have shown that improvements in the execution of the maneuvers were

needed. The third flight campaign consisted of four flights, and the main purpose was to improve the maneuvers execution, with the new slave radio strategy. The flights were planned to be executed in stable and calm atmospheric conditions, aiming not to be influenced by wind, gusts or turbulence, as the OEM does not account for process noise. During the flights, 34 maneuvers were executed according to the planned inputs. Following the flights, the FPR analysis has been executed, to ensure the basis for the following steps.

4.1 Maneuvers execution

In order to evaluate the three different maneuver execution strategies, inputs were given using the radio sticks, a three-position switch and the programmed maneuvers.

Figure 6 shows a stick executed elevator doublet, and it can be seen that this execution has not produced the characteristic steps of the doublet, also being asymmetric. Another side effect was the presence of deflections of the other control surfaces. For the elevator deflection shown in the figure, as the radio control has the input of the elevator and ailerons on the same stick, there are deflections of the ailerons, which might induce coupled dynamics to the lateral-directional modes and flexible modes that are not related directly to the longitudinal dynamics.

For the usage of the three position switch to execute a doublet input, it can be seen in Fig. 7 that there are no more deflections of the other control surfaces, as the pilot executed then hands off, only changing the switch position, but the period of the maneuver was not precise and consistent between different segments.

The programmed maneuvers, however, have been able to achieve the desired deflections and periods, but they were not symmetric, due to an error in the amplitude programmed in the scripts, as can be seen in Fig. 8. It can also be seen that the other surfaces were not neutral. However, those errors were noticed and fixed.

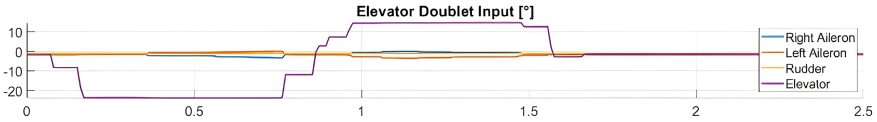

Figure 6. Manual Inputs using Sticks.

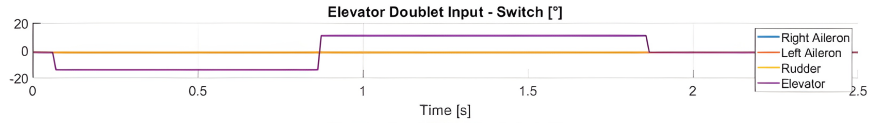

Figure 7. Manual Inputs using Switch.

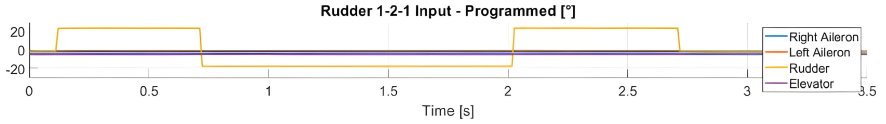

Figure 8. Programmed Input.

4.2 Gathered data and FPR results

For the identification procedure, an overview of the gathered data was done, and with the exception of the extensometers, whose data was contaminated with spikes, the other sensors produced clean signals. The extensometer data will not be used for the FPR analysis, but it is valuable to the model identification accounting for the flexible effects and further analysis must be conducted in the treatment of this signal and the evaluation of the instrumentation system for obtaining a better signal.

To perform the FPR, nine flight segments with lateral-directional and longitudinal excitations performed have been used. Figure 9 shows plots of the airspeed, α, β, Euler's angles, and altitude from the measured flight data and the FPR considering the identified correction factors.

For the attitude variables, it can be seen a good fit between the measured and the reconstructed data, enforcing the assumptions made regarding the IMU data having low influence by the flexibility effects of the airframe. However, the airspeed and angle of attack values do not show a great fitting, even with the estimated correction factors. Furthermore, it was noted during the test flights and the handling of the aircraft that the mounting section of the α and β vanes is subjected to structural deformations during flight, and the classical rigid body kinematics used does not account for those influences, which were though not relevant.

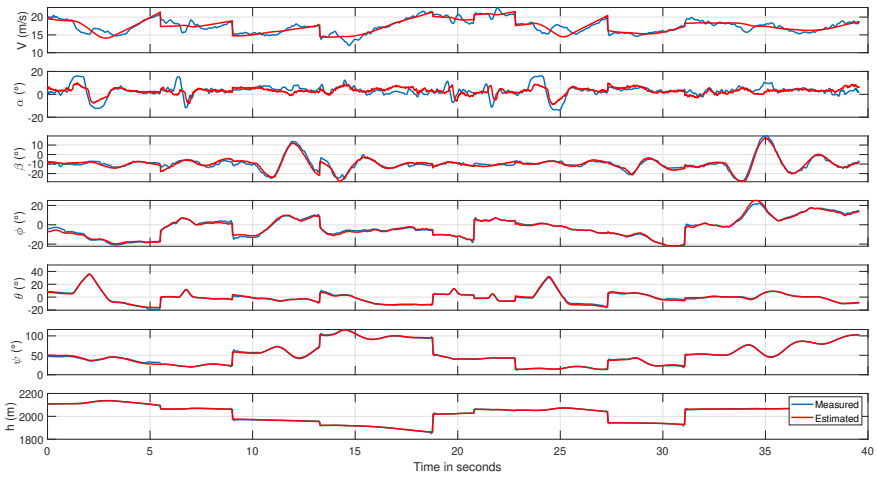

Figure 9. FPR reconstructed data comparison with measured data.

As the aircraft data system has another velocity information, to better evaluate the airspeed of the identified model and its correlation to reality, the velocity measurement of the GNSS system was also compared, which is shown in Fig. 10. It can be seen that the identified model does show an agreement with the GNSS velocity, even though there are errors in some segments, that could be related to imprecision of the measurements and wind influence, as it is important to be explicit that the recorded GNSS speed is not an airspeed, so it was used just as a reference. The GNSS velocity does not clearly depend on α and β, as can be seen in the airspeed measurement. This further indicates to use a better-suited model, including corrections for the structural dynamics and angle of attack and sideslip values, as the airspeed does show dependence on α and β. It is also important to ensure that the flights are not executed in wind presence or with a turbulent atmosphere, as the OEM does not account for that. Besides that, it can be seen from both speed measurements that the model is more related to the VIAS, but it still presents a worse fit than other states.

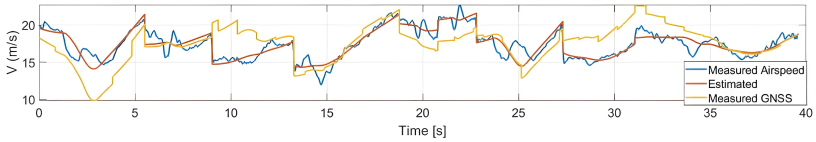

Figure 10. Reconstructed airspeed in comparison with measured data from airspeed and GNSS velocity.

Furthermore, it was also noticed that the trim condition was not met in all the maneuvers. Figure 11 presents an example of a longitudinal dynamics excitation maneuver that started with a banking angle ϕ of almost 10º. The condition for starting the maneuver sequence for the aircraft studied depends on the judgment of the pilot regarding a trimmed start condition and this must be considered in the identification process, as the maneuvers must be checked for the aircraft condition to be in accordance with the expected.

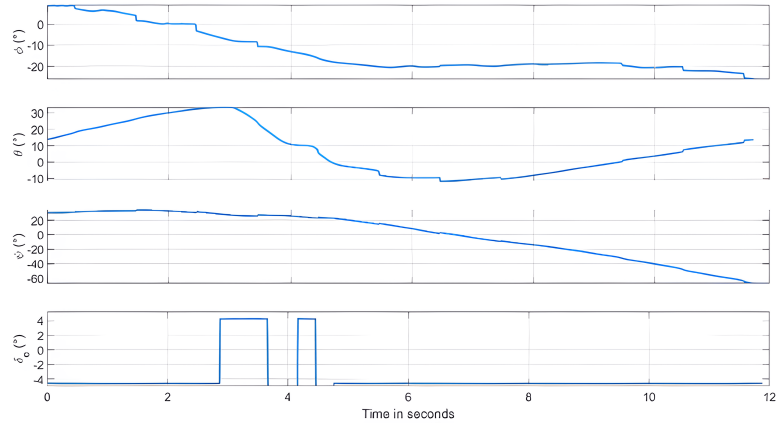

Figure 11. Maneuver executed starting from a non trimmed flight condition.

Finally, it was possible to see improvements over the previously developed works regarding the FPR of the EOLO, and the biggest difference between the reconstructed and measured variables on those were also related to the aerodynamic variables and the anemometric system (Souza *et al.*, 2023). This improvement, obtained by better correction factors, provides more consistent data for the next steps in the identification procedure. However, it is still necessary to improve the results for (α) and airspeed measurements, which means that further development of the aircraft model and refinements over the identification procedure must be done, leading to extended data analysis and the possibility of additional flight campaigns. Another possible approach is to change the position of the angle vanes and pitot tube to provide data with less influence of the aircraft flexibility. Silva (2018) used formulations including the dynamic and static pressure measurements from the anemometric system to achieve a better model for the airspeed calculation accounting for the α and β influence on the pressure measurements, which might provide better results if used with EOLO. One can also analyze synthetically generated α and β values, as another approach to better evaluate those variables. Besides that, the instrumentation system must be inspected and the data produced by the extensometers revised, as it is useful to the next steps of the work expected with this aircraft, the identification of the flexible dynamics model using the flexible aircraft model proposed by Waszak and Schmidt (1988).

5. CONCLUSION

This paper presents the latest findings of a study that utilizes the EOLO UAV to investigate flight dynamics and parameter identification techniques for flexible aircraft. The research was prompted by the need, as indicated by previous results, to obtain more concise data to apply the 4M method. The main obstacle to achieving accurate results was the imprecise inputs that failed to stimulate the aircraft's modes during proposed maneuvers adequately. The forthcoming stages aim to enhance the model by increasing its complexity and including excitations for all relevant modes, so addressing this limitation became essential. To address these challenges, it was proposed to automate the execution of maneuvers and two pilots to conduct the flights. The results demonstrate a significant improvement in maneuver execution and a closer alignment between the Flight Path Recorder (FPR) and the recorded data. This improvement can be attributed to enhanced inputs and the incorporation of additional correction factors. As a consequence, the fidelity of the reconstructed responses has been increased, which permits better data for the subsequent identification steps.

6. REFERENCES

de Paula, T.R., Sarmento, A.G.P., Paixão, V.F., Fisher, C., Machado, R. C., S., A., R.G. and Góes, L.C.S., 2023. "System identification in time domain of flexible aircraft using panel methods". *XII International Conference on Structural Dynamics*.

Deiler, C., Mönnich, W., Seher-Weiß, S. and Wartmann, J., 2023. "Retrospective and recent examples of aircraft and rotorcraft system identification at dlr". *Journal of Aircraft*, Vol. 60, No. 5, pp. 1371–1397. doi:10.2514/1.C037262. URL `https://doi.org/10.2514/1.C037262`.

Grauer, J.A. and Boucher, M., 2020. "System identification of flexible aircraft: Lessons learned from the x-56a phase 1 flight tests". *AIAA Scitech 2020 Forum*. doi:10.2514/6.2020-1017.

Jategaonkar, R.V., 2015. *Flight Vehicle System Identification: A Time Domain Methodology*. USA:AIAA, Reston, VA.

Silva, B.G. and Monnich, W., 2012. "System identification of flexible aircraft in time domain". *AIAA Atmospheric Flight Mechanics*.

Silva, B.G.O., 2018. *System Identification of Flexible Aircraft in Time Domain*. Ph.D. thesis, DLR-Forschungsbericht.

Souza, A.G., Castillo-Zúñiga, D.F., Sarmento, A.G.P., Machado, R.C., Silva, G.A.R. and Goes, L.C.S., 2023. "Data compatibility check of an uas with a flexible wing". *DINAME*, Vol. XIX.

Waszak, M.R. and Schmidt, D.K., 1988. "Flight dynamics of aeroelastic vehicles". *Journal of Aircraft*, Vol. 25, pp. 563–571.

Zuñiga, D.F.C., Souza, A.G. and Góes, L.C.S., 2020. "Flight dynamics modeling of a flexible unmanned aerial vehicle". *Mechanical Systems and Signal Processing*. doi:10.1016/j.ymssp.2020.106900.

Zúñiga, D.F.C., 2019. *Aeroelastic Testing of Flexible Aircraft using Acceleration and Strain Sensors*. Ph.D. thesis, Instituto Tecnológico de Aeronáutica, São José dos Campos, Brasil.

7. RESPONSIBILITY NOTICE

The authors are solely responsible for the printed material included in this paper.